J Biol Inorg Chem (2014) 19:1385–1398
DOI 10.1007/s00775-014-1200-z

ORIGINAL PAPER

Characterization of a lanthanide complex encapsulated with MRI contrast agents into liposomes for biosensor imaging of redundant deviation in shifts (BIRDS)

Samuel Maritim · Yuegao Huang · Daniel Coman · Fahmeed Hyder

Received: 5 May 2014 / Accepted: 23 September 2014 / Published online: 11 October 2014

Abstract Purposely designed magnetic resonance imaging (MRI) probes encapsulated in liposomes, which alter contrast by their paramagnetic effect on longitudinal (T_1) and transverse (T_2) relaxation times of tissue water, hold promise for molecular imaging. However, a challenge with liposomal MRI probes that are solely dependent on enhancement of water relaxation is lack of specific molecular readouts, especially in strong paramagnetic environments, thereby reducing the potential for monitoring disease treatment (e.g., cancer) beyond the generated MRI contrast. Previously, it has been shown that molecular imaging with magnetic resonance is also possible by detecting the signal of non-exchangeable protons emanating from paramagnetic lanthanide complexes themselves [e.g., $TmDOTP^{5-}$, which is a Tm^{3+}-containing biosensor based on a macrocyclic chelate 1,4,7,10-tetraazacyclododecane-1,4,7,10-tetrakis(methylene phosphonate), $DOTP^{5-}$] with a method called biosensor imaging of redundant deviation in shifts (BIRDS). Here, we show that BIRDS is useful for molecular imaging with probes like $TmDOTP^{5-}$ even when they are encapsulated inside liposomes with ultrastrong T_1 and T_2 contrast agents (e.g., Magnevist and Molday ION, respectively). We demonstrate that molecular readouts such as pH and temperature determined from probes like $TmDOTP^{5-}$ are resilient, because the sensitivity of the chemical shifts to the probe's environment is not compromised by the presence of other paramagnetic agents contained within the same nanocarrier milieu. Because high liposomal encapsulation efficiency allows for robust MRI contrast and signal amplification for BIRDS, nanoengineered liposomal probes containing both monomers, $TmDOTP^{5-}$ and paramagnetic contrast agents, could allow high spatial resolution imaging of disease diagnosis (with MRI) and status monitoring (with BIRDS).

Keywords Biosensor imaging of redundant deviation in shifts · Nuclear magnetic resonance · Ligand binding · $TmDOTP5^{-}$

Electronic supplementary material The online version of this article (doi:10.1007/s00775-014-1200-z) contains supplementary material, which is available to authorized users.

S. Maritim (✉) · F. Hyder (✉)
Department of Biomedical Engineering, Yale University, New Haven, CT 06520, USA
e-mail: samuel.maritim@yale.edu

F. Hyder
e-mail: fahmeed.hyder@yale.edu

Y. Huang · D. Coman · F. Hyder
Department of Diagnostic Radiology, Yale University, New Haven, CT, USA

Y. Huang · D. Coman · F. Hyder
Magnetic Resonance Research Center, Yale University, New Haven, CT, USA

D. Coman · F. Hyder
Quantitative Neuroscience with Magnetic Resonance Core Center, Yale University, New Haven, CT, USA

Introduction

Traditional magnetic resonance imaging (MRI) contrast agents, which affect the longitudinal (T_1) and transverse (T_2) relaxation times of tissue water, have improved clinical imaging. Paramagnetic agents such as Magnevist (for T_1) and Molday ION (for T_2) when encapsulated into liposomes can further enhance contrast of the tissue being targeted (e.g., tumor) [1]. However, liposomal research is still in the preclinical stage with potential concerns about

MRI contrast agent stability, which could lead to transmetallation problems in vivo. The goal of these paramagnetic nanoprobes is to generate the strongest contrast possible. Because dynamic range of T_1 contrast enhancement from gadolinium agents is low (i.e., beyond endogenous T_1 contrast), molecular MRI readouts from such agents are difficult. With iron oxide-based T_2 agents, which shorten the T_2 of water due to the magnetic susceptibility field gradients that span large spatial domains to dramatically enhance water relaxation, a molecular readout specific to the local environment of the molecular target becomes challenging. The detection of enhanced water relaxation scheme is further complicated by the fact that T_1 and T_2 agents when encapsulated into nanocarriers develop slightly different properties compared to the bare agent, primarily because of altered water access into the paramagnetic core of the probe [2]. Because of the translational possibilities of MRI technologies, a magnetic resonance method by which molecular readout is possible even in the presence of strong paramagnetic milieu is highly desirable to enable clinical diagnosis in conjunction with monitoring of disease.

It was recently shown that molecular imaging with magnetic resonance is also possible by detecting the chemical shift of non-exchangeable protons (or other nuclei) on paramagnetic lanthanide complexes themselves [e.g., $TmDOTP^{5-}$ and $TmDOTMA^{-}$, which are Tm^{3+}-containing biosensors based on macrocyclic chelates 1,4,7,10-tetraazacyclododecane-1,4,7,10-tetrakis(methylene phosphonate), $DOTP^{5-}$ and 1,4,7,10-tetramethyl-1,4,7,10-tetraazacyclododecane-1,4,7,10-tetraacetate, $DOTMA^{4-}$, respectively] with a method called biosensor imaging of redundant deviation in shifts (BIRDS) [3, 4]. In other words, the BIRDS approach bypasses the need to detect relaxation of abundant water protons, but instead focuses on the chemical shift of dilute non-exchangeable protons on lanthanide complexes such as $TmDOTP^{5-}$ and $TmDOTMA^{-}$. Moderately high-resolution BIRDS data are possible with optimally designed probes and/or improved chemical shift imaging (CSI) schemes [5], because the magnetic resonance properties of the non-exchangeable protons on paramagnetic probes such as $TmDOTP^{5-}$ and $TmDOTMA^{-}$ are quite unusual (e.g., ultrashort relaxation times, highly broadened peaks, hyperfine shifted peaks, etc.).

Probes such as $TmDOTP^{5-}$ and $TmDOTMA^{-}$, and others, have the advantage that the resonances of their non-exchangeable protons have almost no overlap with existing in vivo proton resonances (e.g., water, metabolites, macromolecules) and once detected (i.e., in the order of less than 0.5 mmol/kg), the resonances of these monomers can be used for concentration-independent molecular imaging (e.g., temperature and pH mapping sensitivities with $TmDOTP^{5-}$ do not differ at high or low concentrations) [3, 4]. Furthermore, BIRDS with lanthanide complexes such as $TmDOTP^{5-}$ has the potential for other biomedical applications [e.g., pH/temperature mapping [3, 4] and calibration of chemical exchange saturation transfer (CEST) contrast [6]] using the ^{1}H detection scheme. But if the monomers are modified to include ^{19}F into the chelate, BIRDS could also provide a chemical shift-based alternative to molecular imaging with ^{19}F MRI.

Despite these advantages of BIRDS, monomers such as $TmDOTP^{5-}$ and $TmDOTMA^{-}$ suffer from low spatial resolution CSI voxels (e.g., $\sim$1 μL) compared to MRI voxels (e.g., $\sim$0.1 μL). It should be noted, however, that the best CSI resolution of 1 μL for three-dimensional (i.e., 3D) imaging with BIRDS of the whole rat brain in merely a few minutes that has been achieved with 0.5 mmol/kg of $TmDOTMA^{-}$ [5] can be further improved using faster imaging (e.g., shorter recycle time, faster gradient switching to higher amplitudes, etc.) and increased signal-to-noise ratio (SNR). To improve BIRDS sensitivity further with liposomal encapsulation of the lanthanide monomer (i.e., for improved monitoring of disease status with BIRDS) and considering the possibility of combining BIRDS with other T_1 and T_2 agents typically used for MRI (i.e., to generate superior contrast for disease diagnosis with MRI), we postulated that BIRDS would stand resilient in the presence of large perturbing paramagnetic fields generated by strong T_1 and T_2 contrast agents such as Magnevist and Molday ION, respectively, especially in nanocarriers like liposomes.

The use of liposomes for drug and/or contrast agent delivery is well established [7, 8]. Liposomes can be easily synthesized, they are biocompatible, and their sizes can be readily tailored for biomedical needs. Hydrophilic agents and drugs can be encapsulated in the inner core of the liposomes, while hydrophobic and amphiphilic molecules can be incorporated on to the liposome membrane. Additionally, controlled release [7, 9] in combination with liposome targeting [10–12] can be utilized to reduce unintended side effects of drugs by delivering the drug preferentially to the desired site. Liposomes have recently been used to deliver a high payload of various magnetic resonance agents either encapsulated or incorporated into the liposome membrane for relaxation and sensitivity enhancement [1, 13, 14].

In this work, we report on the utility of BIRDS for molecular imaging with $TmDOTP^{5-}$ in the presence of highly paramagnetic T_1 (Magnevist) and T_2 (Molday ION) contrast agents. We investigated the resiliency of the BIRDS signal for temperature and pH detection with $TmDOTP^{5-}$ co-encapsulated with Magnevist and Molday ION in liposomes. Additionally, we obtained in vitro temperature and pH maps of phantoms containing

$TmDOTP^{5-}$ in the presence of Magnevist and Molday ION in free solution and with liposome encapsulation at different pH values as a precursor to in vivo demonstration of this technology. Overall, these nanoengineered liposomal probes containing $TmDOTP^{5-}$ co-encapsulated with Magnevist and Molday ION show great potential for high spatial resolution imaging of disease diagnosis (with improved contrast for MRI) and status monitoring (with signal amplification for BIRDS).

Materials and methods

Liposome preparation

Liposomes were prepared using the thin film hydration method, where 30 mg of 1,2-dipalmitoyl-sn-glycerophosphocholine (DPPC) was dissolved in 5 mL chloroform, and dried under a gentle stream of nitrogen gas at room temperature to yield a thin film. To remove residual chloroform, the thin film was dried under strong vacuum for at least 6 h at room temperature. The dry film was hydrated at 55 °C for 45 min with varying concentrations of $TmDOTP^{5-}$ (0.25, 1, 2, 5, 10, 25, and 100 mM) in phosphate buffer solution (PBS) at the desired pH (ranging from 6.5 to 8.0). The resulting liposomal suspension was vortexed vigorously and subjected to seven freeze–thaw cycles, alternating between dry ice and a 55 °C water bath. The liposomal suspension (2 mL) was then dialyzed twice using a 2000 MWCO regenerated cellulose (RC) dialysis membrane in 1 L of isotonic NaCl solution (the required tonicity was calculated based on $TmDOTP^{5-}$ concentration) and left to be stirred for 24 h at 4 °C. The NaCl solution was replaced after 24 h with another 1 L NaCl solution of the same tonicity and stirred for another 24 h at 4 °C. This procedure removes almost completely the un-encapsulated $TmDOTP^{5-}$ by diluting its concentration by a factor equal to 250,000 (= $(1{,}000/2)^2$). Thus, the NMR signal of $TmDOTP^{5-}$ after dialysis represents exclusively the encapsulated $TmDOTP^{5-}$. The dialyzed liposomes were then subjected to a 10 min (bath) sonication at 35 °C.

The resulting liposomes were extruded sequentially through polycarbonate filters of different pore sizes (100–800 nm; starting from the larger to the smaller diameter filters) at 55 °C at least 15 times for each filter size. The liposomes were then cooled to room temperature. Liposome size was measured by dynamic light scattering (DLS) using a Malvern Zetasizer Nano ZS instrument with Malvern disposable cuvettes (Malvern USA). Several types of DPPC liposomes were made: liposomes containing only 20 mM $TmDOTP^{5-}$ and 20 mM $TmDOTP^{5-}$ co-encapsulated with either Magnevist (0.5–10 mM) or Molday ION (3.5–35 mg/kg Fe). $TmDOTP^{5-}$ samples in the presence of varying concentrations of Magnevist (0.5–10 mM) and Molday ION (3.5–35 mg/kg Fe) in free solution (i.e., without encapsulation) were also prepared to assess the effect of increasing concentrations of these paramagnetic MRI contrast agents. We measured time-dependent release of $TmDOTP^{5-}$ from liposomes. The $TmDOTP^{5-}$ signal was measured after the first dialysis. The same sample was dialyzed again after 1 year and the $TmDOTP^{5-}$ signal measured again. The $TmDOTP^{5-}$ signal (i.e., concentration) change after 1 year was expressed as a percentage of the first measurement.

Characterization of BIRDS properties

All free solution and liposome-encapsulated samples were characterized for their temperature and pH-dependent BIRDS properties for different MRI contrast agent concentrations. The pH of each sample was measured with a pH meter (Corning 430, NY, USA) using a glass electrode (5 × 178 mm, Calomel, Beckman, Fullerton, CA, USA). ^1H spectra were acquired on an 11.7T Bruker (Billerica, MA, USA) vertical-bore spectrometer between 25 and 40 °C for all samples and fit to a Lorentzian lineshape. The spectra were line broadened (50 Hz), phased (zeroth order), and baseline corrected (first order). Temperature and pH sensitivities of the non-exchangeable protons of $TmDOTP^{5-}$ were fit to a second-order polynomial model that includes temperature (T), pH and chemical shift (δ) [4].

T_1 and T_2 values for H2, H3 and H6 protons of $TmDOTP^{5-}$ (Fig. 1) were obtained at 35 °C using standard inversion recovery and spin-echo sequences, respectively, using several delays of 0.02–10 ms in increments of 0.1 ms for T_1 and 0.2–3 ms in increments of 0.1 ms for T_2, because the intrinsic T_1 and T_2 relaxation times of the non-exchangeable protons of monomers such as $TmDOTP^{5-}$ are very short [4]. The resulting time-dependent intensities were fitted to single exponentials to obtain T_1 and T_2 for each resonance. T_1 and T_2 relaxation times for H2, H3 and H6 protons of $TmDOTP^{5-}$ samples in the presence of varying concentrations of Magnevist (0.5–10 mM) and Molday ION (3.5–35 mg/kg Fe) in free solution and with liposome encapsulation were also determined to assess the effect of increasing concentrations of these paramagnetic MRI contrast agents.

In vitro phantoms for CSI and MRI experiments

Parallel glass tubes containing 0.6 mL samples of known concentrations and pH (see below) were placed in a falcon tube filled with deionized water. The sample tubes were arranged so as to have alternating higher (∼pH 7.6) and lower pH (∼pH 7.0) values. The sample tubes were held in

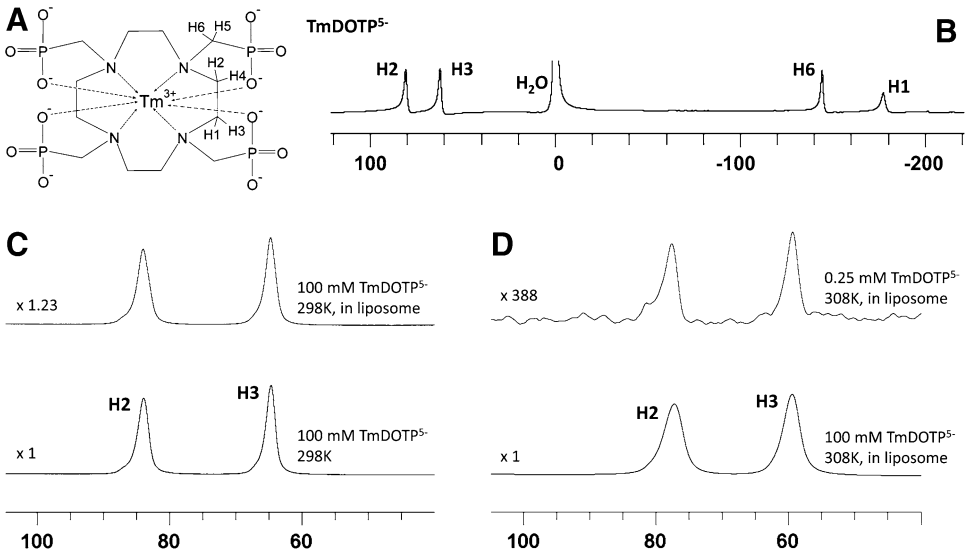

Fig. 1 Encapsulation efficiency and signal amplification of $TmDOTP^{5-}$ in liposomes. **a** Structure of $TmDOTP^{5-}$, where H1–H6 are non-exchangeable protons. **b** ^{1}H spectrum of $TmDOTP^{5-}$, where H1, H2, H3 and H6 protons are detectable within ±200 ppm of water. **c** Comparison of H2 and H3 signal intensities of 100 mM $TmDOTP^{5-}$ shows the intensity in free solution is ×1.23 that of a liposome sample, which represents encapsulation efficiency of 81 % and where the liposome was composed of DPPC (see text). **d** Comparison of H2 and H3 signal intensities for 0.25 and 100 mM $TmDOTP^{5-}$ in liposome shows signal amplification of ×388, which represents about 97 % signal enhancement from the low to high concentration. See Supplementary Figure 1, demonstrating details on further liposome characterization

place by a polystyrene stopper that had holes specially prepared to fit the glass tubes tightly. Sample temperatures were measured before and after the CSI experiment.

In vitro CSI of $TmDOTP^{5-}$

25 × 25 × 25 3D CSI datasets of phantoms were obtained on a 9.4T Agilent horizontal-bore spectrometer using a ^{1}H radio frequency (RF) volume coil (4 cm diameter). A similar experimental setup was used for liposome-encapsulated samples. Two 3D CSI datasets of $TmDOTP^{5-}$ were acquired for each phantom, one with the transmitter offset at +30 kHz from water frequency, (to selectively excite the H2 and H3 resonances) and the other with the transmitter offset at −65 kHz (to selectively excite the H6 resonance). The excitation of H2, H3 and H6 protons was achieved using a single-banded refocused 90° Shinnar-Le Roux (SLR) RF pulse of 30 kHz bandwidth and 300 μs duration. The CSI datasets were acquired using reduced spherical encoding with uniform sampling of *k*-space with 1,743 encoding steps [5] with a recycle time (TR) of 8 ms, 32 averages per encoding step, 2,048 points per FID and a field of view (FOV) of 32 × 32 × 32 mm^3. The phase encode gradient duration was 136 μs and the spectral window was 192 kHz. The spectrum for each encoding step was line broadened (50 Hz), phased (zero order), and baseline corrected (first order). The temperature and pH maps were calculated according to the model described previously [3, 4].

In vitro T_1 and T_2 mapping of water

Water-based T_1 and T_2 maps were acquired on the 9.4T Agilent spectrometer using the ^{1}H RF volume coil (4 cm diameter). A spin-echo MRI pulse sequence was used to image a 128 × 128 slice of 2 mm thickness with 32 × 32 mm^2 FOV. For T_1 mapping, five different TR values were used (0.4, 0.7, 1, 2 and 5 s), while for T_2 mapping, ten different echo time (TE) values were used (in the range from 7 to 70 ms, with 7 ms increments). The T_1 and T_2 values were calculated by fitting the absolute intensity to a single exponential function.

Results

Encapsulation efficiency and signal amplification with liposomal BIRDS

Figure 1a, b, respectively, shows the structure and assignments of four (H1, H2, H3 and H6) of the six non-exchangeable protons of $TmDOTP^{5-}$, which are based on 2D NMR assignments of the chelate, but the hyperfine shifted signals of the complex can be easily distinguished by 1D NMR as well [15]. The spectrum was truncated to exclude the signals from the two protons farthest from the water resonance, H4 and H5 (+500 and −385 ppm respectively). $TmDOTP^{5-}$ was successfully encapsulated in

the liposomes and exhaustive dialysis was carried out to remove the non-encapsulated $TmDOTP^{5-}$ (see "Methods" for detailed description). The encapsulation efficiency of the liposomes was determined by comparing the signal intensities, given by the area under the resonances (which is T_2 independent) of the H2 and H3 protons of the liposomal $TmDOTP^{5-}$ against the areas of the corresponding signals in the free solution $TmDOTP^{5-}$ (i.e., non-encapsulated) as shown in Fig. 1c. The NMR spectra were acquired with very long repetition time (TR = 100 ms) to allow complete T_1 relaxation of all $TmDOTP^{5-}$ protons. Both the encapsulated and the free solution had the same $TmDOTP^{5-}$ concentration of 100 mM. The H2 and H3 intensities of the free solution $TmDOTP^{5-}$ were 1.23 times greater than the corresponding intensities of the liposome-encapsulated $TmDOTP^{5-}$ providing an encapsulation efficiency of 88 %. The utility of the liposome encapsulation for delivering a high local payload of MRI contrast agent was evaluated by comparing the signal intensities of liposome-encapsulated 0.25 and 100 mM $TmDOTP^{5-}$ under the same experimental conditions and acquisition parameters as shown in Fig. 1d. Comparison of H2 and H3 signal intensities (for the 0.25 and 100 mM $TmDOTP^{5-}$ in liposome) shows signal amplification of × 388, which represents about 97 % signal enhancement from the low to the high concentration. We emphasize that the signal enhancement refers to the gain in 'payload' that liposomes can deliver. For example, if 100 mM $TmDOTP^{5-}$ is injected directly into the body the monomer gets diluted with tissue/blood fluids, whereas liposomes encapsulated with 100 mM $TmDOTP^{5-}$ if injected would generate a concentrated (i.e., amplified) signal provided that the monomer is not released from the liposome (see below).

The DPPC liposomes generated from our procedure resulted in a size range of 70–75 nm (Supplementary Figure 1A). A linear dependence was observed for 1–100 mM of $TmDOTP^{5-}$ encapsulated in DPPC liposomes (Supplementary Figure 1B and C). Comparison of the spectra in Fig. 1c, d suggests that the $TmDOTP^{5-}$ signals remain largely unaffected upon liposome encapsulation. Furthermore, the DPPC liposome encapsulated with $TmDOTP^{5-}$ was stable over time (Supplementary Figure 1D). We found that liposomes encapsulated with higher concentration of $TmDOTP^{5-}$ released more of the monomer over a 1-year time period than in the case of liposomes encapsulated with lower concentration of $TmDOTP^{5-}$. While these results suggest that the extra-liposomal release of the monomer is dependent on the initial $TmDOTP^{5-}$ concentration, freshly made liposomes encapsulated with $TmDOTP^{5-}$ could provide maximal payload necessary for in vivo experiments.

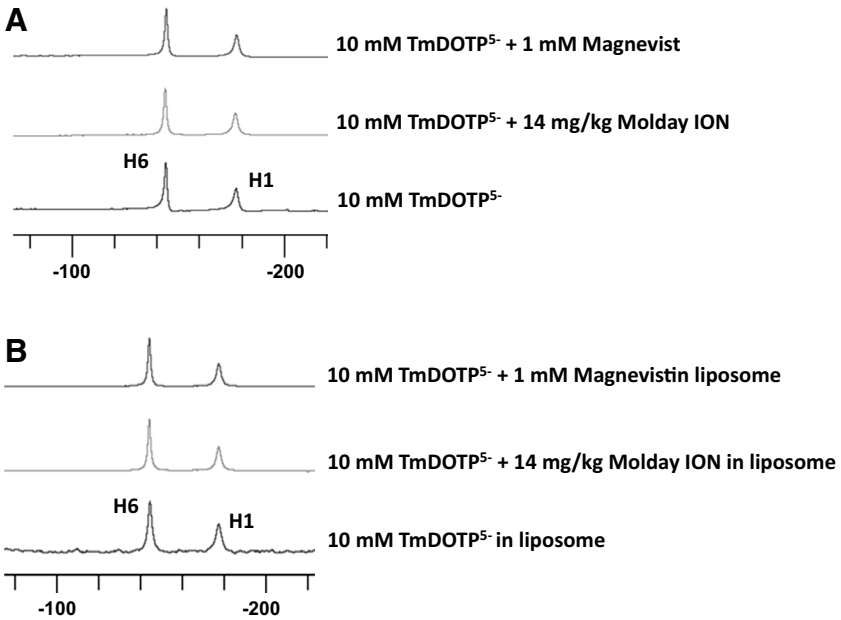

Fig. 2 Resiliency of BIRDS demonstrated with $TmDOTP^{5-}$ in the presence of strong contrast agents in free solution and encapsulated in liposomes. **a** Comparison of H6 and H1 signal intensities of 10 mM $TmDOTP^{5-}$ in free solution (*bottom*) and in the presence of 14 mg/kg Fe in Molday ION (*middle*) or 1 mM Magnevist (*top*). **b** Comparison of H6 and H1 signal intensities of 10 mM $TmDOTP^{5-}$ encapsulated in liposome (*bottom*) and in the presence of 14 mg/kg Fe in Molday ION (*middle*) or 1 mM Magnevist (*top*) within the liposomes. It is evident from comparison of (**a**) and (**b**) that the $TmDOTP^{5-}$ signal (i.e., chemical shift by BIRDS) is resilient even in the presence of strong paramagnetic contrast agents such as Magnevist and Molday ION, regardless of whether the agent is encapsulated or not. All spectra were acquired at 11.7 T, 308 K and pH 7.2

Characterization of BIRDS with and without co-encapsulation of contrast agents

The resiliency of the BIRDS with $TmDOTP^{5-}$ was evaluated in the presence of strong paramagnetic T_1 and T_2 contrast agents (Magnevist and Molday ION respectively), both in free solution and with liposome encapsulation, over a temperature range of 25–40 °C and pH range of 6.5–8.0. Figure 2a, b, respectively, shows ^1H spectra of 10 mM $TmDOTP^{5-}$ samples in the presence of 14 mg/kg Fe of Molday ION or 1 mM Magnevist as free solutions and with liposome encapsulation. Inspection of these spectra suggests that the $TmDOTP^{5-}$ chemical shifts remain largely unaltered by the two MRI contrast agents, regardless of encapsulation. Figure 3a, b shows that pH and temperature sensitivities of the $TmDOTP^{5-}$ signals were not affected (within the experimental error of the measurement) by the presence of the MRI contrast agents or by liposome encapsulation. Therefore, $TmDOTP^{5-}$ can still be used as a dual (temperature and pH) sensor in the presence of these agents at the respective doses. Temperature measured with BIRDS was within 0.1 °C of temperature measured with a thermocouple and pH measured with BIRDS was within 0.1 pH units verified with a pH meter.

Figure 4 shows the effect of the strong paramagnetic MRI contrast agents on BIRDS by independent measures of the linewidths for the non-exchangeable protons of $TmDOTP^{5-}$ when the concentration of the contrast agent was increased, both in free solution and with co-encapsulation. The MRI contrast agents only minimally affected the linewidths of the $TmDOTP^{5-}$ resonances with increasing concentrations of Magnevist (Fig. 4a) and Molday ION (Fig. 4c) in free solution. However, the resonance linewidths increased slightly upon liposome encapsulation with Magnevist (Fig. 4b) and Molday ION (Fig. 4d), but also in the absence of any contrast agent. The small linewidth differences between $TmDOTP^{5-}$ peaks in free solution and in liposome, as shown in Fig. 4, are primarily due to T_2-based line broadening upon encapsulation of the monomer and the contrast agent (see below).

The effect of the strong paramagnetic MRI contrast agents on BIRDS properties were tested by independent measurements of the relaxation times for the non-exchangeable protons when the concentration of the contrast agent was increased, both in free solution and with co-encapsulation, as shown in Fig. 5. Both T_1 and T_2 values in free solution were in the order of 0.5–2.5 ms for $TmDOTP^{5-}$ resonances, either alone or in the presence of Magnevist and Molday ION (Fig. 5a, b). In fact, increasing concentrations of Magnevist and Molday ION in free solution did not significantly affect the T_1 and T_2 values for $TmDOTP^{5-}$ resonances. Upon encapsulation, the T_1 values remained largely unaffected, whereas T_2 values were shortened (Fig. 5c, d). The error bars in Fig. 5 depend on the goodness of exponential fits to the relaxometry data of the non-exchangeable protons of $TmDOTP^{5-}$.

In vitro BIRDS and MRI with and without co-encapsulation of contrast agents

We tested the BIRDS properties of $TmDOTP^{5-}$ in the presence of other contrast agents, both in free solution and with liposome encapsulation. Two phantoms were made, one with $TmDOTP^{5-}$ in free solution (with/without agents) and another with $TmDOTP^{5-}$ encapsulated (with/without agents) under different conditions described below. Each phantom consisted of six glass tubes of 5 mm outer diameter (in clockwise order from a to f in Fig. 6). Figure 6a shows $TmDOTP^{5-}$ in the presence of Magnevist and Molday ION in free solution, where tubes a and b contained 20 mM $TmDOTP^{5-}$ at pH 7.7 and 7.0, respectively; c and d contained 10 mM $TmDOTP^{5-}$ with 14 mg/kg of Fe in Molday ION at pH 7.6 and 6.8, respectively; e and f contained 10 mM $TmDOTP^{5-}$ with 1 mM Magnevist at pH 7.5 and 6.8, respectively. Figure 6b shows $TmDOTP^{5-}$ encapsulated into liposome with Magnevist and Molday ION, where tubes a and b contained 20 mM $TmDOTP^{5-}$ at pH 7.6 and 7.0, respectively; c and d contained 10 mM $TmDOTP^{5-}$ with 14 mg/kg of Fe in Molday ION at pH 7.6 and 6.9, respectively; e and f contained 10 mM $TmDOTP^{5-}$ with 1 mM Magnevist at pH 7.6 and 7.0, respectively.

Temperature and pH measured by BIRDS showed excellent agreement (less than 0.1 °C for temperature and less than 0.1 units for pH) with independent temperature and pH measurements by thermocouple and pH meter, respectively, regardless of the presence of contrast agents with $TmDOTP^{5-}$ in free solution (Fig. 6a) or co-encapsulation of $TmDOTP^{5-}$ with other contrast agents into liposomes (Fig. 6b). Temperature maps of the phantoms showed that all bottles had the same temperature, 20 °C for the free solution phantom in Fig. 6a and 22 °C for the liposome-encapsulated phantoms in Fig. 6b. Importantly, temperature and pH determination were not affected by the presence of paramagnetic MRI contrast agents or by encapsulation. For the same phantoms shown in Fig. 6, we also measured the water relaxation properties (Supplementary Figure 2). Imaging of the phantoms with standard inversion recovery (for T_1) and spin-echo (for T_2) sequences showed R_1 (i.e., $= 1/T_1$) enhancement with Magnevist and R_2 (i.e., $= 1/T_2$) enhancement with Molday ION. The relaxation enhancements were pH independent for the samples in free solution, while the encapsulated samples showed pH-dependent relaxation enhancements, except for the samples containing Molday ION.

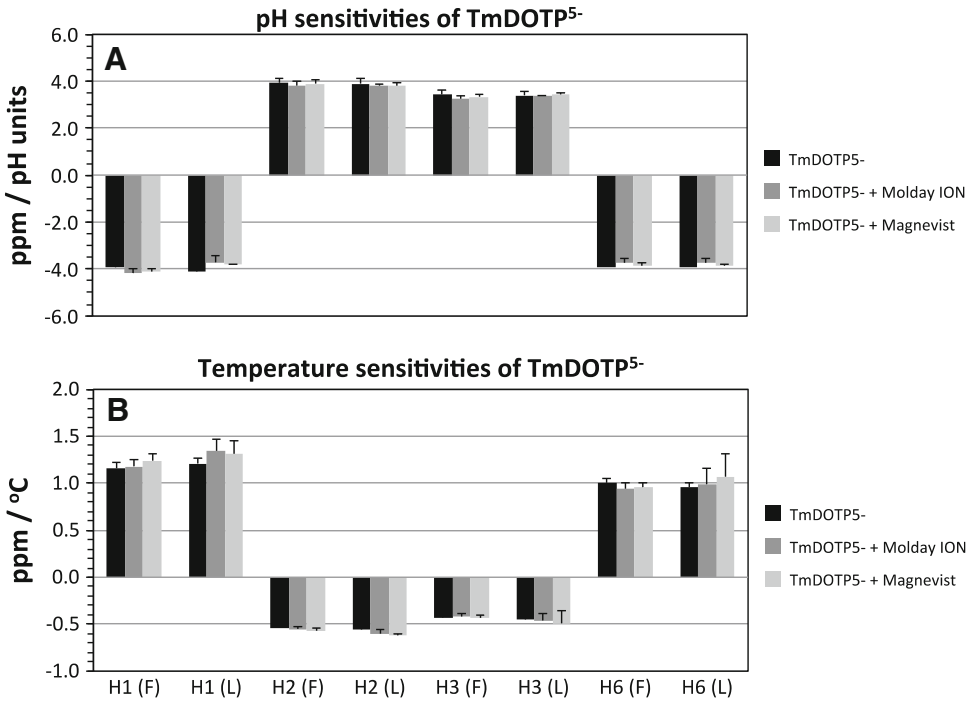

Fig. 3 Temperature and pH sensitivities of $TmDOTP^{5-}$ in free solution and liposome encapsulation in the presence of T_1 and T_2 contrast agents. **a** Comparison of pH sensitivities for H1, H2, H3 and H6 protons of 10 mM $TmDOTP^{5-}$ in the presence of 14 mg/kg of Fe in Molday ION and 1 mM Magnevist in free solution (F) and under liposome encapsulation (L). The pH sensitivities are not affected much by Molday ION or Magnevist. **b** Comparison of temperature sensitivities for H1, H2, H3 and H6 protons of 10 mM $TmDOTP^{5-}$ in the presence of 14 mg/kg of Fe in Molday ION and 1 mM Magnevist in free solution (F) and under liposome encapsulation (L). The temperature sensitivities are not significantly affected by Molday ION or Magnevist

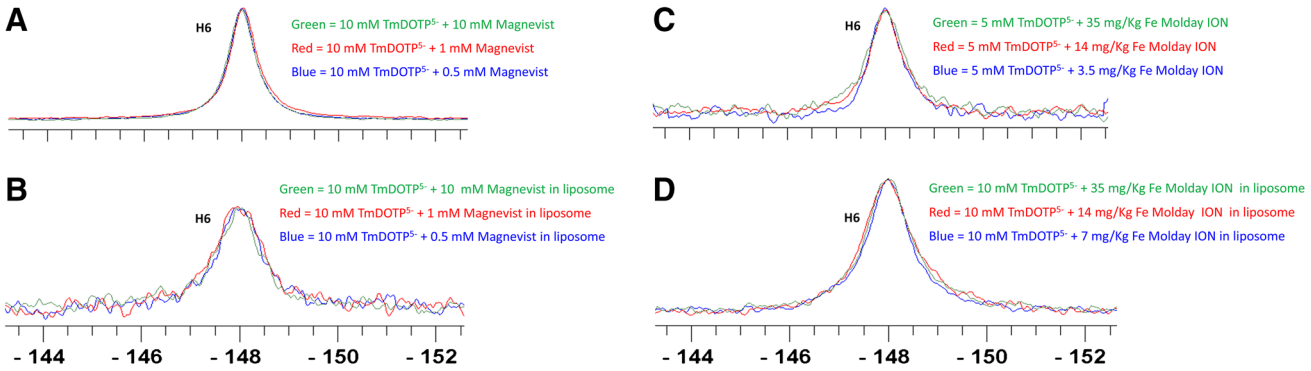

Fig. 4 Impact on line broadening of $TmDOTP^{5-}$ protons assessed by varying concentrations of strong contrast agents (i.e., Magnevist and Molday ION) in free solution and encapsulated in liposomes. **a** Comparison of H6 signal intensities of 10 mM $TmDOTP^{5-}$ in free solution in the presence of 0.5 mM (*blue*), 1 mM (*red*) and 10 mM (*green*) Magnevist. The full width at half maximum (FWHM) values of the three spectra are in the range of 340–350 Hz, with the broadest FWHM at the highest contrast agent dose. **b** Comparison of H6 signal intensities of 10 mM $TmDOTP^{5-}$ encapsulated within liposomes in the presence of 0.5 mM (*blue*), 1 mM (*red*) and 10 mM (*green*) Magnevist. The FWHM values of the three spectra are in the range of 390–480 Hz, with the broadest FWHM at the highest contrast agent dose. **c** Comparison of H6 signal intensities of 5 mM $TmDOTP^{5-}$ in free solution in the presence of 3.5 mg/kg (*blue*), 14 mg/kg (*red*) and 35 mg/kg (*green*) of Fe in Molday ION. The FWHM values of the three spectra are in the range of 370–420 Hz, with the broadest FWHM at the highest contrast agent dose. **d** Comparison of H6 signal intensities of 10 mM $TmDOTP^{5-}$ encapsulated within liposomes in the presence of 3.5 mg/kg (*blue*), 14 mg/kg (*red*) and 35 mg/kg (*green*) of Fe in Molday ION. The FWHM values of the three spectra are in the range of 410–510 Hz, with the broadest FWHM at the highest contrast agent dose. Comparison of (**a**) and (**c**) suggests minimal line broadening with Magnevist and Molday ION, but comparison of (**b**) and (**d**) suggests some degree of line broadening upon encapsulation

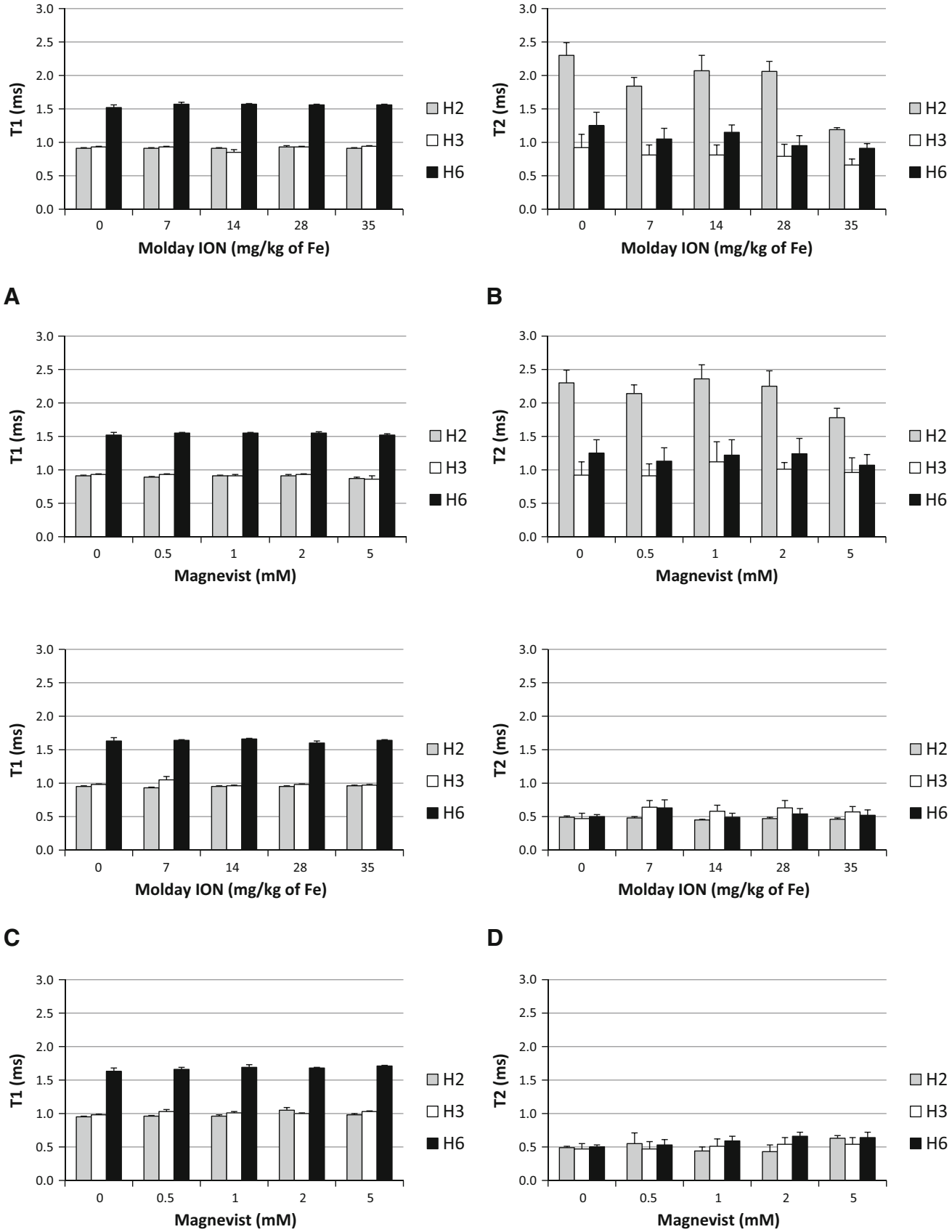
A
B
C
D
T1 (ms)
T2 (ms)
H2
H3
H6
Molday ION (mg/kg of Fe)
Magnevist (mM)
0
7
14
28
35
0.5
1
2
5
0.0
0.5
1.0
1.5
2.0
2.5
3.0

◀**Fig. 5** Impact on relaxation times of $TmDOTP^{5-}$ protons assessed by varying concentrations of strong contrast agents (i.e., Magnevist and Molday ION) in free solution and encapsulated in liposomes. Comparison of **a** T_1 and **b** T_2 values for H2 (*gray*), H3 (*white*) and H6 (*black*) signals of 10 mM $TmDOTP^{5-}$ in free solution with increasing concentrations of Molday ION (*top*) and Magnevist (*bottom*). Comparison of **c** T_1 and **d** T_2 values for H2 (*gray*), H3 (*white*) and H6 (*black*) signals of 10 mM $TmDOTP^{5-}$ encapsulated within liposomes with increasing concentrations of Molday ION (*top*) and Magnevist (*bottom*). In free solution, while Magnevist does not seem to affect T_2 values for the $TmDOTP^{5-}$ protons significantly, at the highest Molday ION concentrations the T_2 values for the $TmDOTP^{5-}$ protons are marginally attenuated. However upon encapsulation, both the contrast agents significantly affect the T_2 values of the TmDOTP5 protons without affecting the temperature and pH sensitivities

Discussion

A continuing challenge in molecular imaging of disease (e.g., cancer) diagnosis is the need for non-invasive and translational magnetic resonance methods that will allow for quantitative monitoring of tissue status prior to, during and following treatment, in addition to high-resolution contrast imaging. A probe that will report on the local environment and physiology (e.g., temperature and pH) of the tumor and its microscopic location is thus highly desirable for clinical applications. Temperature and pH imaging with lanthanide complexes like $TmDOTP^{5-}$ has previously been demonstrated in vitro and in vivo using BIRDS [3–6]. While we used $TmDOTP^{5-}$ as a model monomer in this study for liposomal BIRDS, we expect that other paramagnetic (i.e., lanthanide or transition) metal complexes would provide similar results.

However, BIRDS with monomer provides low SNR because of the low local concentration detected. In this work, we sought to amplify the BIRDS signal through encapsulation of a high payload of $TmDOTP^{5-}$ in liposomes and achieved a signal amplification of ×388 using nanomolar amounts of liposome (Fig. 1). $TmDOTP^{5-}$ was

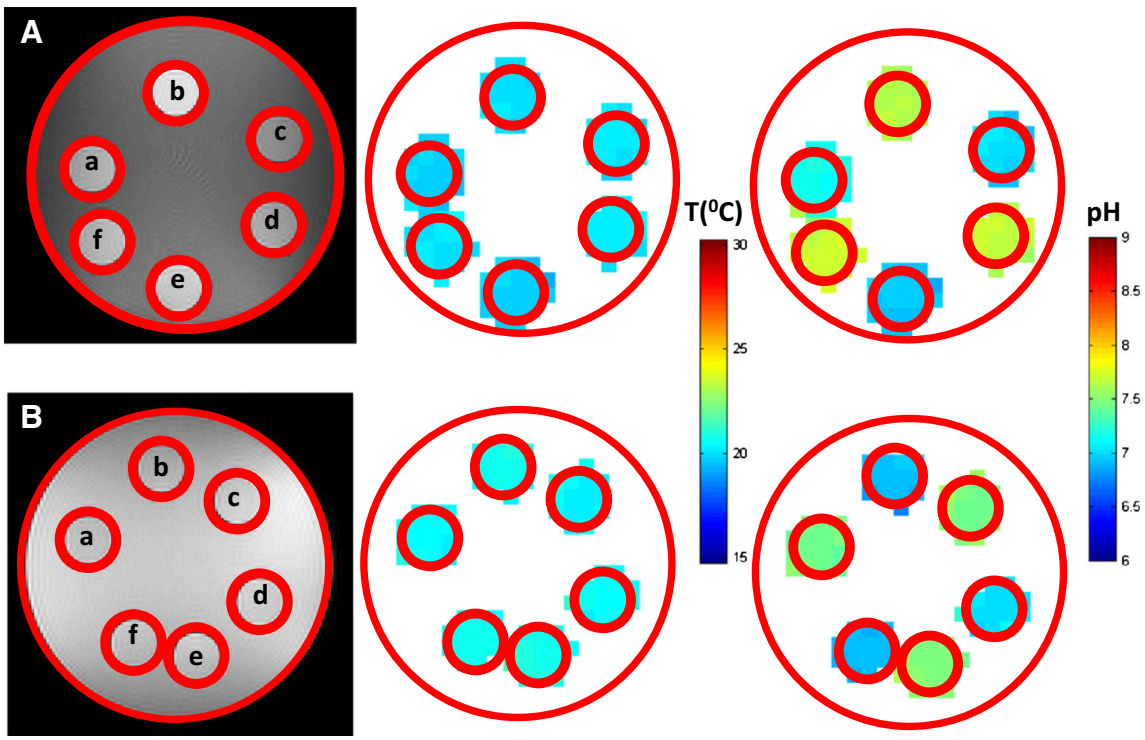

Fig. 6 In vitro temperature and pH maps from BIRDS using $TmDOTP^{5-}$ either in (**a**) free solution or (**b**) encapsulated in liposomes. **a** Comparison of BIRDS data from different bottle phantoms with 20 mM $TmDOTP^{5-}$ in free solution at pH 7.0 in bottle *a* and at pH 7.7 in bottle *b*, 10 mM $TmDOTP^{5-}$ in free solution with 14 mg/kg of Fe in Molday ION at pH 6.8 in bottle *c* and at pH 7.6 in bottle *d*, and 10 mM $TmDOTP^{5-}$ in free solution with 1 mM Magnevist at pH 6.8 in bottle *e* and at pH 7.5 in bottle *f*. Thus, bottles *a*–*f* had pH values of 7.6, 7.0, 7.6, 6.8, 7.5 and 6.8, respectively, but each bottle contained $TmDOTP^{5-}$ in free solution with or without a contrast agent. **b** Comparison of BIRDS data from different bottle phantoms with 20 mM $TmDOTP^{5-}$ encapsulated in liposomes at pH 7.6 in bottle *a* and at pH 7.0 in bottle *b*, 10 mM $TmDOTP^{5-}$ in free solution with 14 mg/kg of Fe in Molday ION at pH 7.6 in bottle *c* and at pH 6.9 in bottle *d*, and 10 mM $TmDOTP^{5-}$ in free solution with 1 mM Magnevist at pH 7.6 in bottle *e* and at pH 7.0 in bottle *f*. Thus, bottles *a*–*f* had pH values of 7.6, 7.0, 7.6, 6.9, 7.6 and 7.0, respectively, but each bottle contained $TmDOTP^{5-}$ encapsulated in liposomes with or without a contrast agent. Regardless of whether $TmDOTP^{5-}$ was encapsulated or not, the BIRDS data showed that all bottles had approximately the same measured temperature given that they were all imaged at the same room temperature, which was ~20 °C for (**a**) and ~22 °C for (**b**), whereas the measured pH values were within 0.1 pH units of the actual pH in each bottle. See Supplementary Figure 2 for water proton relaxation data acquired for these phantoms

successfully co-encapsulated with Magnevist and Molday ION in DPPC-based liposomes with high encapsulation efficiency (Supplementary Figure 1). BIRDS signal was found to be resilient even in the presence of strong MRI contrast agents such as Magnevist and Molday ION, whether they were encapsulated or not (Fig. 2). Molecular readouts of pH and temperature from $TmDOTP^{5-}$ were not significantly compromised by the presence of other paramagnetic agents, either in free solution or when encapsulated into liposomes (Fig. 3).

Upon liposome encapsulation, regardless of contrast agent that was co-encapsulated, the BIRDS properties were slightly affected (Figs. 4, 5), as the $TmDOTP^{5-}$ resonances were broadened due to T_2 shortening. The T_2 decrease of the $TmDOTP^{5-}$ resonances upon encapsulation is probably due to enhanced spin–spin interaction mediated by longer correlation times arising with compartmentalization of $TmDOTP^{5-}$ molecules inside the liposomes. While the shortened T_2 values lead to broader signals and thus render these signals insensitive to static magnetic field inhomogeneity (i.e., shim insensitive), the short T_1 values can be utilized for rapid signal averaging enabling higher SNR. However, the molecular imaging capability of $TmDOTP^{5-}$ in the presence of MRI contrast agents with BIRDS remained promising regardless of liposome encapsulation (Fig. 6). Additionally, relaxation enhancements of bulk water (i.e., R_1 and R_2) were achieved with Magnevist and Molday ION, respectively, for improved MRI contrast (Supplementary Figure 2). However, R_1 enhancements with Magnevist and R_2 enhancements with Molday ION observed with $TmDOTP^{5-}$ in free solution were attenuated when encapsulated into liposomes. This is probably due to exchange-limited relaxation processes in liposomes, whereby membrane impermeability makes the paramagnetic liposome core less accessible to bulk water. Exchange-limited relaxation has previously been observed for MRI contrast agents encapsulated in liposomes made from saturated lipids [2, 16].

Unconventional properties of BIRDS for molecular imaging

The BIRDS scheme is unusual because in molecular MRI the norm is to detect the paramagnetic contrast agent's effect on relaxation rates of water protons. The BIRDS platform is an ultrahigh speed, high spatial resolution, 3D CSI mode where the paramagnetically shifted and non-exchangeable protons from lanthanide (or transition) metal complexes are detected. These protons have extremely short relaxation times (to allow high-speed CSI signal averaging) and their shifts are sensitive reporters of ambient conditions (to allow molecular sensing by CSI). The distinctiveness of BIRDS, compared to other MRI or MRS methods used for biosensing [17–21], is based on specific properties that these protons possess. The proton resonances are paramagnetically shifted away from the chemical shift of water protons and thus the signals are easily detected by CSI without any need for water suppression or outer volume suppression. All such lanthanide (and transition metal) complexes report data on temperature, whereas complexes with phosphonate pendant arms [e.g., $DOTP^{8-}$ [4] or $DOTA4AmP^{8-}$ [22]] report on both temperature and pH. Because lanthanide monomers like $TmDOTP^{5-}$ can reach the brain's interstitial space [23], they report extracellular pH. Temperature and/or pH sensitivities of these paramagnetic complexes are notably better than with other diamagnetic MRS methods [3, 4, 24–30].

The T_1 and T_2 of the paramagnetically shifted protons are significantly shortened such that the $\sqrt{(T_2/T_1)}$ ratio, which is a crucial factor in SNR for all MRI and MRS methods, begins to approach unity. In comparison, the $\sqrt{(T_2/T_1)}$ ratio for diamagnetic proton signals is in the range of 0.01–0.1 [31]. Thus, high spatial resolution CSI is possible with BIRDS [3–5]. Signal averaging is enhanced without cost of additional acquisition time, because T_1 of paramagnetically shifted protons is usually a few ms. In comparison, T_1 of diamagnetic protons is in the order of 10^3 ms. Thus ultrahigh speed CSI is possible with BIRDS. The paramagnetically shifted protons are impervious to static magnetic field inhomogeneities (i.e., shim) because T_2 is less than a few ms. In contrast, T_2 of diamagnetic protons is 10^1–10^2 ms and thus are susceptible to poor shim conditions. Thus, no additional shimming is needed for BIRDS. Since the paramagnetically shifted signals do not overlap with other endogenous or exogenous diamagnetic proton signals, the BIRDS detection scheme requires little further calibration or optimization. Because multiple protons are detected from a monomer simultaneously and each has slightly different sensitivity to the same molecular event, redundant detection improves the accuracy for temperature and/or pH mapping [4]. Finally, because the BIRDS detection scheme is purely based on chemical shift, the molecular reporting by BIRDS is independent of complex concentration, blood flow and/or metabolism. Thus, detection of signals from a monomer such as $TmDOTP^{5-}$ is quantitative with BIRDS under most circumstances as long as a reliable MRS signal is detected.

Resiliency of BIRDS in highly paramagnetic environments

The current results demonstrate that lanthanide complexes such as $TmDOTP^{5-}$ manifest similar BIRDS properties regardless of the presence of strong MRI contrast agents (e.g., Magnevist and Molday ION) and liposome

encapsulation. To understand how BIRDS properties remain essentially unaffected in such dire situations when usually the water proton relaxation rates are dramatically affected, the mechanisms that underlie the unusual properties of protons on monomers like $TmDOTP^{5-}$ need to be discussed.

The paramagnetic core of monomers such as $TmDOTP^{5-}$ is similar to the paramagnetic center in a protein, as protons of both complexes interact with the unpaired electrons of the metal ion [15, 32, 33]. Because these effects mainly depend on the distance and orientation between the proton nuclear spin and the lanthanide (or transition) metal ion, structural attributes of the complexes can be gathered from contributions to the relaxation rate and the chemical shift of the nuclear spins. In fact, it is the structural manifestations of the monomer responding to the immediate environment changes that enable BIRDS. If the paramagnetic center possesses magnetic susceptibility anisotropy (i.e., departure of the susceptibility tensor from symmetry and as is the case for lanthanide ions, except for paramagnetic gadolinium and diamagnetic lanthanide ions), then the proton nuclear spin features enhanced relaxation rates in conjunction with the so-called hyperfine shifts. A key feature of BIRDS (i.e., where protons attached to the monomer itself are detected) is that the paramagnetic effect of the metal ion on the protons for complexes such as $TmDOTP^{5-}$ is constant (i.e., pseudo-static), a property which arises from the kinetic stability and in vivo inertness of such complexes under a variety of conditions [34].

The magnetic susceptibility of a substance (i.e., potential for it to interact with a magnetic field) is the sum of diamagnetic and paramagnetic terms. The diamagnetic term can be neglected for small complexes such as $TmDOTP^{5-}$, but this term cannot be ignored for repetitive ring systems that stack up (e.g., DNA or RNA). Thus the paramagnetic term, which is the main contributor to the anisotropy, dominates in complexes such as $TmDOTP^{5-}$. The fixed spatial proximity of the proton nuclear spin to the unpaired electrons severely enhances the transverse relaxation rate (i.e., $1/T_2$) via dipolar and Curie-spin contributions, enough to induce line broadening ($\Delta\nu_{1/2}$),

$$\begin{aligned}\pi \cdot \Delta\nu_{1/2} &= \frac{1}{T_2} \\ &= \left\{\left(f\left(\gamma_H^2, \ldots\right) \cdot \tau_S / r^6\right) + \left(f\left(\omega_H^2, \ldots\right) \cdot \tau_R / r^6\right)\right\} \\ &\geq \frac{1}{T_1} \end{aligned} \quad (1)$$

where γ_H and ω_H are, respectively, the gyromagnetic ratio and Larmor frequency of protons, τ_S is the electron spin relaxation time (about 0.1 ps), τ_R is the re-orientational correlation time of the complex (about 80 ps) and r is the proton–metal distance (about 10^{-2}–10^{-1} nm). Equation 1 shows that the dependence of $\Delta\nu_{1/2}$ on the inverse sixth power for r dictates a highly irrepressible effect compared to other effects. Previously, it was shown that monomers such as $TmDOTP^{5-}$ demonstrate a very mild dependence on the static magnetic field, ranging from 4 to 11.7 T [4]. In the current study we observed that T_1 of the monomer's protons are unaltered significantly by different ambient conditions [i.e., T_1 of the free complex in solution and T_1 of the complex in presence of strong paramagnetic agents (regardless of liposomal encapsulation) are quite similar], whereas T_2 of the monomer's protons are just as resilient except that they shorten with liposomal encapsulation. We believe that the T_2 shortening with encapsulation is primarily due to increased correlation times (see above), which is expected due to restricted molecular motion, an effect that depends on liposome size (see below).

The paramagnetic effect of the metal ion on the protons of monomers such as $TmDOTP^{5-}$ also dictates the hyperfine shifts of the complex because of the fixed spatial orientation between the proton and the unpaired electrons. The hyperfine shifts have two contributions: the contact shift observed at very short distances around the metal ion and the pseudo-contact shift whose orientation and distance dependence over longer distances can also reveal structural features. Lanthanide complexes such as $TmDOTP^{5-}$ generally depend on pseudo-contact shifts, although the presence of both effects is possible in specific scenarios. Since the effect on chemical shift depends on a set vector L between the proton and the unpaired electrons, factors such as temperature and pH affecting L will influence the shift. Thus, variation of the total shift term for a given proton, $\Delta\delta_o$, with both temperature (T) and pH (ignoring other effects) is then given by

$$\Delta\delta_o = C_T \cdot \Delta T + C_{pH} \cdot \Delta pH \quad (2)$$

where $C_T = (\Delta\delta_o/\Delta T)_{pH}$ is the temperature dependence of chemical shift at a given pH and $C_{pH} = (\Delta\delta_o/\Delta pH)_T$ is the pH dependence of chemical shift at a given temperature. Equation 2 shows that if the main determinants of the chemical shift effect (i.e., C_T and C_{pH}) are dominated by fixed (i.e., pseudo-static) interactions, similar to the relaxation enhancements, then the biosensing properties are likely to be resilient over a wide range of conditions as long as the complex is kinetically stable. In the current study, we observed that temperature and/or pH sensitivities of the monomer's protons are practically unchanged by different ambient conditions [i.e., BIRDS properties of the free complex in solution and BIRDS properties of the complex in presence of strong paramagnetic agents (regardless of liposomal encapsulation) are quite similar]. This stands in contrast to water relaxation-based temperature detection, as Hijnen et al. [35] recently reported that temperature

dependence of water proton shifts induced by Gd-DTPA is −0.00038 ppm/mM/ °C. In our case, the most concentrated Magnevist (i.e., 10 mM) would afford about 0.0038 ppm/ °C, which is negligible compared to the BIRDS sensitivities for the protons of $TmDOTP^{5-}$. Small changes in pH sensitivities, especially in the case of liposomal encapsulation, might be due to the low permeability of the membrane and/or slow water exchange, a property that can be modified with materials used to make the liposome (see next section).

The fact that the BIRDS properties of the protons on $TmDOTP^{5-}$ are not significantly affected by the presence of strong MRI contrast agents (at doses equal to or higher than used in preclinical molecular imaging research) suggests that interaction between the chelate proton and the paramagnetic field of the chelate metal is much stronger than the interaction between the chelate proton and the paramagnetic field of the MRI contrast agent. It does not seem that $TmDOTP^{5-}$ and the MRI contrast agents are in direct contact, because the measured properties of the monomer under various experimental conditions do not suggest that the monomer and the agent are linked by hydrogen bonding and/or electrostatic forces. The interaction between the chelate proton and the paramagnetic field of the chelate metal is likely to be very strong for two reasons: first, the effect occurs over short distances (i.e., in the order of 10^{-2}–10^{-1} nm); second, the effect is static (i.e., the complex is kinetically stable in solution). Alternatively, the interaction between the chelate proton and the paramagnetic field of the MRI contrast agent is likely to be weaker in comparison, because the two interacting moieties are much farther away (i.e., in the order of 10^{-1}–10^{0} nm) and probably tumbling at different time constants. This type of space–time paramagnetic interaction for shift and relaxation effects has been explained by the hard sphere model [36]. However, the bulk magnetic susceptibility shifts created by the MRI contrast agents may not be ignored if their concentrations are substantially high [37].

Considerations of lipid type and size

The relaxation enhancement of $TmDOTP^{5-}$ resonances that was observed upon encapsulation can be explained by an exchange-limited relaxation process, whereby diffusion of water molecules across the DPPC liposome membrane is decreased. Formulation of liposomes with lipids that are more permeable will not only improve the relaxivity of the encapsulated contrast agent, but also the ability to report on the molecular environment. Fossheim and colleagues characterized the effect of lipid type (which affects water permeability) and liposome size and showed that R_1 was enhanced with decreasing liposome size and degree of lipid unsaturation [2, 38]. The enhanced R_1 with increased permeability and small size of liposome suggests an exchange-limited relaxation process.

Castelli et al. [10] showed that R_2 enhancement of a lanthanide-encapsulating liposome could be improved by incorporating an amphiphilic lanthanide complex on the liposome membrane and by increasing the size of the liposome. Larger liposomes have higher magnetic susceptibility, because they are able to encapsulate a higher amount of contrast agent and thus have higher transverse relaxivity. On this basis, it may be expected that encapsulation (and incorporation on the lipid bilayer) of neutral (or hydrophobic) agents will allow for encapsulation (or incorporation) of a larger amount of agent and thus enhance the relaxivities even further.

The drawback to increasing the liposome size to enhance sensitivity is that at larger sizes, liposome clearance by the reticuloendothelial system is increased [39]. The problem of reticuloendothelial system clearance can be reduced by specially formulating the liposomes by steric stabilization, e.g., with polyethylene glycol (PEG) and cholesterol. Lokling et al. [16] improved the stability of the pH-sensitive dipalmitoyl phosphatidylethanolamine/palmitic acid (DPPE/PA) liposomal GdDTPA-BMA (previously shown to be unstable in blood) by incorporating cholesterol onto the membrane. Incorporation of cholesterol had the added effect of reducing pH sensitivity of the liposome. However, they showed that replacing the palmitic acid (PA) with the unsaturated amphiphile dipalmitoylsuccinylglycerol (DPSG) made the liposomes stable in blood and more pH sensitive. Steric stabilization of liposomes by incorporation of PEG has been shown to result in liposomes with higher plasma stability and increased circulation time [40]. However, a potential drawback of increasing the liposome size is reduced accessibility of the nanoparticle to tissular and/or interstitial domains for pH or temperature mapping. Thus, nanoprobes like these would provide vascular physiology at best. However with liposome surface modification, the nanoprobes could be designed for extravascular targets.

Active targeting of liposomes

Active targeting of liposomes co-encapsulating drugs, monomers with BIRDS capability and MRI contrast agents could allow for the delivery as well as quantitative monitoring of the effects of a drug treatment non-invasively at high resolution. Through active targeting, smaller amounts of drug or contrast agent can be used to achieve the same or even higher accumulation in tissue relative to unencapsulated or encapsulated, but untargeted agents [41]. Additionally, the use of targeted liposomes will reduce cytotoxicity and undesired side effects that would otherwise result from stochastic distribution of the agents or

drugs. Glutamine-functionalized liposomes encapsulating Dy-DTPA-BMA have previously been used for monitoring liposomal drug release and accumulation in vivo [10]. Flament et al. [13] demonstrated lipoCEST effect using RGD-conjugated thulium (4,7-bis-carboxymethyl-1,4,7,10-tetraaza-cyclododec-1-yl)-acetic acid liposome composed of 32:5:58:5 POPC:DOPG:Chol:DSPE-PEG. Liver targeting with gadolinium-labeled liposomes containing the amphiphile Gd-DTPA derivatives of varying chains has also been reported [42]. Active targeting of liposomes in such a manner may allow for the potential utility in image-guided drug delivery [43] and monitoring disease status prior to, during and following treatment for longitudinal study without the need of invasive surgical procedures (or animal killing).

Summary

Nanomolar liposome formulations encapsulating a high payload of $TmDOTP^{5-}$ were prepared and their BIRDS properties examined. $TmDOTP^{5-}$ signal was shown to be resilient, while BIRDS temperature and pH sensitivities were insignificantly affected by co-encapsulation of $TmDOTP^{5-}$ in the presence of strong paramagnetic agents such as Magnevist and Molday ION inside liposomes. At constant $TmDOTP^{5-}$ concentration, increasing concentrations of the co-encapsulated MRI contrast agents do not affect the relaxation times and linewidths of the non-exchangeable protons of $TmDOTP^{5-}$. Formulation of liposomes with lipids that are more permeable will not only improve the water relaxivity of the encapsulated agents, but also the ability to report on the molecular environment. Because all contrast agents and liposome formulations used herein have previously been used in vivo, this work should be translatable. This molecular imaging platform may allow for in vivo image-guided drug delivery, whereby hydrophilic drugs are co-encapsulated with the contrast agents, while hydrophobic drugs may be incorporated into the liposome membrane. Additionally, amphiphilic $TmDOTP^{5-}$-like monomers may be incorporated on to the liposome membrane to enhance sensitivity and/or avoid reacting with encapsulated drugs.

Acknowledgments The study was supported by NIH Grants (R01 CA-140102, R01 EB-011968, P30 NS052519).

References

1. Strijkers GJ, Mulder WJ, van Heeswijk RB, Frederik PM, Bomans P, Magusin PC, Nicolay K (2005) Relaxivity of liposomal paramagnetic MRI contrast agents. Magma 18:186–192
2. Fossheim SL, Fahlvik AK, Klaveness J, Muller RN (1999) Paramagnetic liposomes as MRI contrast agents: influence of liposomal physicochemical properties on the in vitro relaxivity. Magn Reson Imaging 17:83–89
3. Coman D, Trubel HK, Hyder F (2010) Brain temperature by biosensor imaging of redundant deviation in shifts (BIRDS): comparison between TmDOTP5- and TmDOTMA. NMR Biomed 23:277–285
4. Coman D, Trubel HK, Rycyna RE, Hyder F (2009) Brain temperature and pH measured by (1)H chemical shift imaging of a thulium agent. NMR Biomed 22:229–239
5. Coman D, de Graaf RA, Rothman DL, Hyder F (2013) In vivo three-dimensional molecular imaging with biosensor imaging of redundant deviation in shifts (BIRDS) at high spatiotemporal resolution. NMR Biomed 26:1589–1595
6. Coman D, Kiefer GE, Rothman DL, Sherry AD, Hyder F (2011) A lanthanide complex with dual biosensing properties: CEST (chemical exchange saturation transfer) and BIRDS (biosensor imaging of redundant deviation in shifts) with europium DOTA-tetraglycinate. NMR Biomed 24:1216–1225
7. Hagtvet E, Evjen TJ, Olsen DR, Fossheim SL, Nilssen EA (2011) Ultrasound enhanced antitumor activity of liposomal doxorubicin in mice. J Drug Target 19:701–708
8. Krause W, Klopp R, Leike J, Sachse A, SchuhmannGiampieri G (1995) Liposomes in diagnostic imaging—comparison of modalities—in-vivo visualization of liposomes. J Lipos Res 5:1–26
9. Staruch R, Chopra R, Hynynen K (2011) Localised drug release using MRI-controlled focused ultrasound hyperthermia. Int J Hyperth 27:156–171
10. Castelli DD, Terreno E, Cabella C, Chaabane L, Lanzardo S, Tei L, Visigalli M, Aime S (2009) Evidence for in vivo macrophage mediated tumor uptake of paramagnetic/fluorescent liposomes. NMR Biomed 22:1084–1092
11. Mulder WJ, Strijkers GJ, Griffioen AW, van Bloois L, Molema G, Storm G, Koning GA, Nicolay K (2004) A liposomal system for contrast-enhanced magnetic resonance imaging of molecular targets. Bioconjug Chem 15:799–806
12. Paulis LE, Jacobs I, van den Akker NM, Geelen T, Molin DG, Starmans LW, Nicolay K, Strijkers GJ (2012) Targeting of ICAM-1 on vascular endothelium under static and shear stress conditions using a liposomal Gd-based MRI contrast agent. J Nanobiotechnol 10:25
13. Flament J, Geffroy F, Medina C, Robic C, Mayer JF, Meriaux S, Valette J, Robert P, Port M, Le Bihan D, Lethimonnier F, Boumezbeur F (2013) In vivo CEST MR imaging of U87 mice brain tumor angiogenesis using targeted LipoCEST contrast agent at 7 T. Magn Reson Med 69:179–187
14. Yang Y, Schuhle DT, Dai G, Alford JK, Caravan P (2012) 1H chemical shift magnetic resonance imaging probes with high sensitivity for multiplex imaging. Contrast Media Mol Imaging 7:276–279
15. Geraldes CF, Sherry AD, Lazar I, Miseta A, Bogner P, Berenyi E, Sumegi B, Kiefer GE, McMillan K, Maton F et al (1993) Relaxometry, animal biodistribution, and magnetic resonance imaging studies of some new gadolinium (III) macrocyclic phosphinate and phosphonate monoester complexes. Magn Reson Med 30:696–703
16. Lokling KE, Skurtveit R, Bjornerud A, Fossheim SL (2004) Novel pH-sensitive paramagnetic liposomes with improved MR properties. Magn Reson Med 51:688–696
17. Hashim AI, Zhang X, Wojtkowiak JW, Martinez GV, Gillies RJ (2011) Imaging pH and metastasis. NMR Biomed 24:582–591
18. Perez-Mayoral E, Negri V, Soler-Padros J, Cerdan S, Ballesteros P (2008) Chemistry of paramagnetic and diamagnetic contrast

agents for magnetic resonance imaging and spectroscopy pH responsive contrast agents. Eur J Radiol 67:453–458
19. Ward KM, Aletras AH, Balaban RS (2000) A new class of contrast agents for MRI based on proton chemical exchange dependent saturation transfer (CEST). J Magn Reson 143:79–87
20. Zhang Y, Poirer-Quinot M, Springer CS Jr, Balschi JA (2010) Discrimination of intra- and extracellular 23Na+ signals in yeast cell suspensions using longitudinal magnetic resonance relaxography. J Magn Reson 205:28–37
21. Zhou J, Lal B, Wilson DA, Laterra J, van Zijl PC (2003) Amide proton transfer (APT) contrast for imaging of brain tumors. Magn Reson Med 50:1120–1126
22. Huang Y, Coman D, Ali MM, Hyder F (2014) Lanthanide ion (III) complexes of 1,4,7,10-tetraazacyclododecane-1,4,7,10-tetraaminophosphonate (DOTA-4AmP8-) for dual biosensing of pH with CEST (chemical exchange saturation transfer) and BIRDS (biosensor imaging of redundant deviation in shifts). Contrast Media Mol Imaging (in press)
23. Trubel HKF, Maciejewski PK, Farber JH, Hyder F (2003) Brain temperature measured by H-1-NMR in conjunction with a lanthanide complex. J Appl Physiol 94:1641–1649
24. Brugge JF, Poon PW, So AT, Wu BM, Chan FH, Lam FK (1995) Thermal images of somatic sensory cortex obtained through the skull of rat and gerbil. Exp Brain Res 106:7–18
25. De Poorter J, De Wagter C, De Deene Y, Thomsen C, Stahlberg F, Achten E (1995) Noninvasive MRI thermometry with the proton resonance frequency (PRF) method: in vivo results in human muscle. Magn Reson Med 33:74–81
26. Evanochko WT, Ng TC, Glickson JD, Durant JR, Corbett TH (1982) Human tumors as examined by in vivo 31P NMR in athymic mice. Biochem Biophys Res Commun 109:1346–1352
27. Garcia-Martin ML, Herigault G, Remy C, Farion R, Ballesteros P, Coles JA, Cerdan S, Ziegler A (2001) Mapping extracellular pH in rat brain gliomas in vivo by 1H magnetic resonance spectroscopic imaging: comparison with maps of metabolites. Cancer Res 61:6524–6531
28. Gatenby RA, Gillies RJ (2004) Why do cancers have high aerobic glycolysis? Nature reviews. Cancer 4:891–899
29. Gillies RJ, Liu Z, Bhujwalla Z (1994) 31P-MRS measurements of extracellular pH of tumors using 3-aminopropylphosphonate. Am J Physiol 267:C195–C203
30. Gillies RJ, Raghunand N, Garcia-Martin ML, Gatenby RA (2004) pH imaging. A review of pH measurement methods and applications in cancers. IEEE Eng Med Biol Mag 23:57–64
31. de Graaf RA, Brown PB, McIntyre S, Nixon TW, Behar KL, Rothman DL (2006) High magnetic field water and metabolite proton T1 and T2 relaxation in rat brain in vivo. Magn Reson Med 56:386–394
32. Casellato U, Tamburini S, Tomasin P, Vigato PA, Aime S, Botta M (1999) Synthesis, X-ray structure, and solution nmr studies of Ln(III) complexes with a macrocyclic asymmetric compartmental schiff base. preference of the Ln(III) ions for a crown-like coordination site. Inorg Chem 38:2906–2916
33. Koehler J, Meiler J (2011) Expanding the utility of NMR restraints with paramagnetic compounds: background and practical aspects. Prog Nucl Magn Reson Spectrosc 59:360–389
34. Sherry AD, Caravan P, Lenkinski RE (2009) Primer on gadolinium chemistry. J Magn Reson Imaging 30:1240–1248
35. Hijnen NM, Elevelt A, Pikkemaat J, Bos C, Bartels LW, Grull H (2013) The magnetic susceptibility effect of gadolinium-based contrast agents on PRFS-based MR thermometry during thermal interventions. J Ther Ultrasound 1(1):8
36. Welti DH, Linder M, Ernst RR (1978) Comparison of molecular geometries determined by paramagnetic nuclear magnetic-resonance relaxation and shift-reagents in solution. J Am Chem Soc 100:403–410
37. Chu SCK, Xu Y, Balschi JA, Springer CS (1990) Bulk magnetic-susceptibility shifts in nmr-studies of compartmentalized samples—use of paramagnetic reagents. Magn Reson Med 13:239–262
38. Fossheim SL, Colet JM, Mansson S, Fahlvik AK, Muller RN, Klaveness J (1998) Paramagnetic liposomes as magnetic resonance imaging contrast agents. Assessment of contrast efficacy in various liver models. Invest Radiol 33:810–821
39. Abra RM, Hunt CA (1981) Liposome disposition invivo. 3. dose and vesicle-size effects. Biochim Biophys Acta 666:493–503
40. Slepushkin VA, Simoes S, Dazin P, Newman MS, Guo LS, de-Lima MCP, Duzgunes N (1997) Sterically stabilized pH-sensitive liposomes—intracellular delivery of aqueous contents and prolonged circulation in vivo. J Biol Chem 272:2382–2388
41. Papahadjopoulos D, Kirpotin DB, Park JW, Hong KL, Shao Y, Shalaby R, Colbern G, Benz CC (1998) Targeting of drugs to solid tumors using anti-HER2 immunoliposomes. J Lipos Res 8:425–442
42. Kabalka GW, Davis MA, Holmberg E, Maruyama K, Huang L (1991) Gadolinium-labeled liposomes containing amphiphilic Gd-Dtpa derivatives of varying chain-length—targeted mri contrast enhancement agents for the liver. Magn Reson Imaging 9:373–377
43. Li C, Penet MF, Winnard P Jr, Artemov D, Bhujwalla ZM (2008) Image-guided enzyme/prodrug cancer therapy. Clin Cancer Res 14:515–522